ACADEMIA ROMÂNĂ
Revue Roumaine de Chimie
https://www.icf.ro/rrch/

Rev. Roum. Chim.,
2023, *68*(1–2), 49–59
DOI: 10.33224/rrch.2023.68.1-2.05

STRUCTURAL CHARACTERIZATION AND ANTIMICROBIAL ACTIVITY OF 2-[4,6-(Cl/CH_3/CF_3)-BENZIMIDAZOL-2-YL]-4-(OCH_3/Br)-PHENOLS AND THEIR Zn(II), Pd(II) AND Au(III) COMPLEXES

Aydin TAVMAN,[a,*] Ayşe Zuhal ELMAL,[b] Demet GÜRBÜZ,[a] Mayram HACIOGLU,[c] A. Seher BIRTEKSÖZ TAN[c] and Adem ÇINARLI[a]

[a] Istanbul University-Cerrahpaşa, Faculty of Engineering, Department of Chemistry, 34320, Avcilar, Istanbul, Turkey
[b] Istanbul University-Cerrahpaşa, Institute of Graduate Education, Department of Chemistry, 34320, Avcilar, Istanbul, Turkey
[c] Istanbul University, Faculty of Pharmacy, Department of Pharmaceutical Microbiology, 34452, Beyazit, Istanbul, Turkey

Received December 1, 2022

2-[4,6-{Dichloro/dimethyl/bis-(trifluoromethyl)}-benzimidazol-2-yl]-(5-bromo/methoxy)-phenols (**HL_1** – **HL_6**) and their complexes with $ZnCl_2$, $PdCl_2$ and $AuCl_3$ were synthesized and characterized. The structures of the complexes were confirmed on the basis of elemental analysis, molar conductivity, FT-IR, NMR and fluorescence spectroscopy. Most of the complexes are four-coordinated with a 1:2 M:L ratio and the Au(III) complexes are 1:1 electrolyte whereas the others are non-electrolyte. According to the fluorescence spectra, electronegative substituents such as bromo, chloro, trifluoromethyl and methoxy were found to increase red shift (shifting to higher wavelength). The highest wavelength was observed to belong to **HL_6** (trifluoromethyl-methoxy derivative) with 531 nm. When compared to the ligands, there is a decrease in the red shift and fluorescence intensity in the spectra of the complexes. In addition, antimicrobial activity of the compounds was evaluated against six bacteria and three fungi. The Au(III) complexes have superior activity against all the bacteria, while the Pd(II) complexes showed higher antifungal activity than the ligands and metal salt.

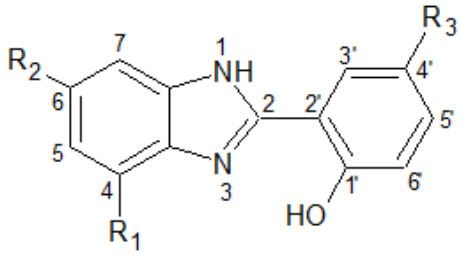

INTRODUCTION

Various benzimidazole derivatives play the role of active ingredient of many drugs in the field of pharmacology. Many researchers continue their research in this field, especially due to the fact that it has a wide variety of biological activities such as antimicrobial, antiviral, antifungal, antiulcer, anti-inflammatory, pancreatic lipase inhibitor, proton pump inhibitor, antihypertensive, antidiabetic, hormone modulator, antidepressant, anticoagulant, etc.[1-7] Many types of benzimidazole derivatives are known to have biological activity. For example, the structure of vitamin B12 includes a 5,6-dimethylbenzimidazole moiety, which is coordinated to a Co(II) ion.[8,9]

Ozegowski and Krebs synthesized a compound called Bendamustine (4-{5-[bis(2-chloroethyl) amino]-1-methyl-2-bezimidazolyl}butyric acid hydrochloride) for the first time in 1963, which is a benzimidazole-containing drug with anticancer property.[10,11] Bendamustine, which is sold and used under trade names such as Treanda and Ribomustin, is a chemotherapy medication used in the treatment of chronic lymphocytic leukemia (CLL)[12], multiple myeloma[13], and non-Hodgkin's lymphoma.[14,15]

Benzimidazole derivatives containing hydroxyphenyl group are compounds that are one of the current and very common research topics and the results of which have the opportunity to be applied in many fields.[16] One of the most important features of these compounds is that they are strong

* Corresponding author: atavman@iuc.edu.tr (A. Tavman)

chelating compounds (ligands) with two ring structures, benzimidazole and phenol ring, over OH oxygen and C=N nitrogen. On the other hand, benzimidazolylphenols and their complexes are known to have a wide range of antimicrobial activity, and many studies have been published both by us and other researchers in this area.[17-25] For example, the Hg(II) and Ag(I) complexes of 2-(5-nitro-1*H*-benzimidazol-2-yl)-4-bromophenol were found to have superior activity toward the microorganisms whereas the Pd(II) and Cd(II) complexes showed considerably antimicrobial effect on *S. aureus* and *C. albicans* selectively.[25]

In this study, six new benzimidazolylphenol derivatives, 2-[4,6-{Dichloro/dimethyl/bis-(trifluoromethyl)}-benzimidazol-2-yl]-(5-bromo/methoxy)-phenols (**HL$_1$** – **HL$_6$**, Figure 1) and their complexes with $ZnCl_2$, $PdCl_2$ and $AuCl_3$ were synthesized and characterized. In addition, antimicrobial activities of the compounds were tested towards six bacteria and three fungi. The structural characteristics and antimicrobial activity of the complexes were investigated and compared.

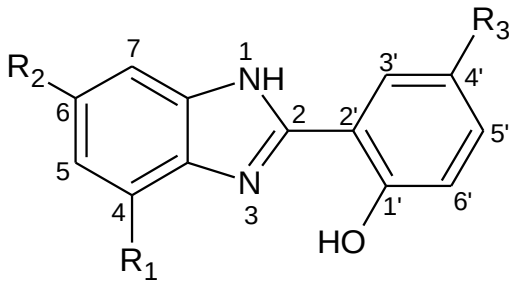

Fig. 1 – Chemical structure of the ligands (**HL$_1$** – **HL$_6$**).

R_1=R_2= CH_3, R_3=Br (**HL$_1$**) R_1=R_2= CH_3, R_3=OCH_3 (**HL$_4$**)
R_1=R_2= Cl, R_3=Br (**HL$_2$**) R_1=R_2= Cl, R_3=OCH_3 (**HL$_5$**)
R_1=R_2= CF_3, R_3=Br (**HL$_3$**) R_1=R_2= CF_3, R_3=OCH_3 (**HL$_6$**)

RESULTS AND DISCUSSION

In this study, eighteen related transition metal complexes were obtained by allowing the ligands to react with Zn(II), Pd(II) and Au(III) ions at a molar ratio of 1:1. Synthesis of the Pd(II) and Au(III) complexes was performed in ethanol, the Zn(II) complexes in ethylacetate, and no pH measurement or adjustment was made. Hence, the factors such as characteristics of the ligand, metal salts and solvent are decisive on complex formation.

The solubility of ligands is good in polar solvents, but poor in non-polar solvents. The solubility of the complexes in polar solvents is mediocre and almost insoluble in non-polar solvents.

The M:L ratio is 1:1 in [Pd(**HL$_1$**)Cl_2]·H_2O, [Au(**HL$_1$**)Cl_3]·H_2O, [Au(**HL$_5$**)Cl_3]·$4H_2O$ and [Pd(**HL$_6$**)Cl_2] complexes**,** it was determined as 1:2 in the others. It is interesting that the 1:1 ones are the Pd(II) and Au(III) complexes. The Zn(II) and Pd(II) complexes are non-electrolyte whereas the Au(III) complexes are 1:1 electrolyte according to the molar conductivity measurements in DMF according to Geary.[26]

Infrared spectroscopy

IR spectroscopy data of the obtained compounds are presented in Experimental section. In the IR spectra of the ligands (**HL$_1$** – **HL$_6$**), the stretching vibrational bands of NH and OH groups are seen above 3100 cm^{-1} and stretching vibrational bands of aromatic CH bonds between 3050 and 3100 cm^{-1}. In the ligands, broad (wide) bands are also observed between 3200 and 2800 cm^{-1}, which is thought to be due to the presence of intramolecular and intermolecular hydrogen bonds. Moderate bands between 1610 and 1640 cm^{-1} are considered to belong to C=N bond stretching vibrations (ν), while bands between 1580 to 1610 cm^{-1} are considered to belong to stretching vibrations of C=C bonds.[17,27] In addition, the bands, which are mostly severe in character between 740 and 850 cm^{-1}, are thought to be caused by the out-of-plane stretching of aromatic CH bonds (δ(CH)). In addition, vibrational bands of aryl C–Cl and C–Br bonds in the compounds are detected in the ranges of 760–545 cm^{-1} and 650–500 cm^{-1}, respectively. Aliphatic C–F bonds (CF_3) present in **HL$_3$** and **HL$_6$** were observed as intense bands between 1060 and 1150 cm^{-1}.[28]

The remarkable changes in complex compounds compared to ligands are as follows: Due to the coordination over C=N nitrogen and OH oxygen atoms in the complexes, the disappearance of OH bands around 3200 cm^{-1} and significant changes in the frequency and character of the C=N bands were observed. The coordination of imine nitrogen atom could also be confirmed by appearance of new bands with medium absorption around 620 and 690 cm^{-1} may be assignable to ν(M–N) vibration modes.[29,30]

^{1}H-NMR Spectroscopy

^{1}H-NMR spectroscopy data of the obtained compounds are given in Experimental section. In the ^{1}H-NMR spectra of the compounds, NH and OH protons appear above 12 ppm, and aromatic ring protons signals are seen in the range of 7 to

8.5 ppm. It could be followed whether the phenolic OH protons are removed by complexation or not in the ^{1}H-NMR spectra. In the Pd(II) and Au(III) complexes, the chemical shift values of the ligand protons are observed to be shifts to a significantly higher ppm value (downfield shift), while the shifts in the Zn(II) complexes are lower, weak and limited, albeit in the same direction.

All the ligands can be considered as dibasic acids and the OH and NH protons may be dissociated in suitable solvent or media. Thus, both protons in **HL$_5$** could not be detected in the NMR spectrum because they were bound by strong hydrogen bonds and were easily dissociated as a result. It is known that metal ions are also effective on deprotonation. Deprotonation was observed in the Zn(II) complexes mostly. This different behavior of the Zn(II) complexes can be explained by the fact that Zn(II) is a softer acid than the other metal ions.

According to the ^{1}H-NMR spectra, the compounds **HL$_1$**, **HL$_2$** and **HL$_4$** have isomeric structures as shown in Figure 2. ^{1}H-NMR spectra of **HL$_2$** is presented in Figure 3.

Fluorescence spectroscopy

Fluorescence spectroscopy data of the compounds obtained are included in Experimental section. It was observed that the wavelengths of the emission spectrum increase (redshift) in sequence of **HL$_1$**, **HL$_2$** and **HL$_3$** (dimethyl, dichloro, bis(trifluoromethyl) derivatives): 459, 485 and 497 nm, respectively in ethanol. In other words, when the electronegativity of the substituents increases, the red shift in the emission spectra of the compounds increases. When the fluorescence effect of substitutions is compared, it is seen that the methoxy group increases the red shift, that is, the wavelength values of the emission spectrum increase. The wavelength values are 514 and 531 nm for **HL$_5$** and **HL$_6$**, respectively (methoxy-trifluoromethyl and methoxy-chloro derivatives), whereas the 459–497 nm is the range for **HL$_1$**, **HL$_2$**, **HL$_3$** and **HL$_4$** (Fig. 4). In addition, **HL$_5$** and **HL$_6$** showed dual fluorescence characteristics.

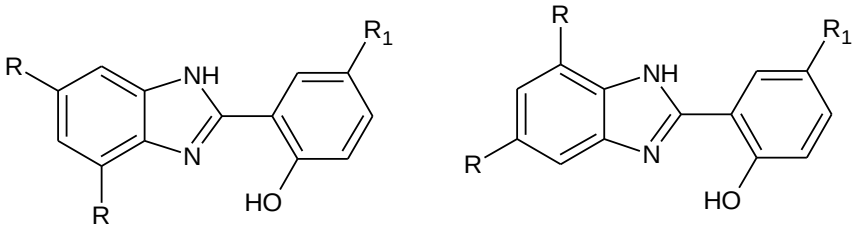

Fig. 2 – Isomeric structures of **HL$_1$** (R = CH_3, R_1 = Br), **HL$_2$** (R = Cl, R_1 = Br) and **HL$_4$** (R = CH_3, R_1 = OCH_3) according to the ^{1}H-NMR spectral data.

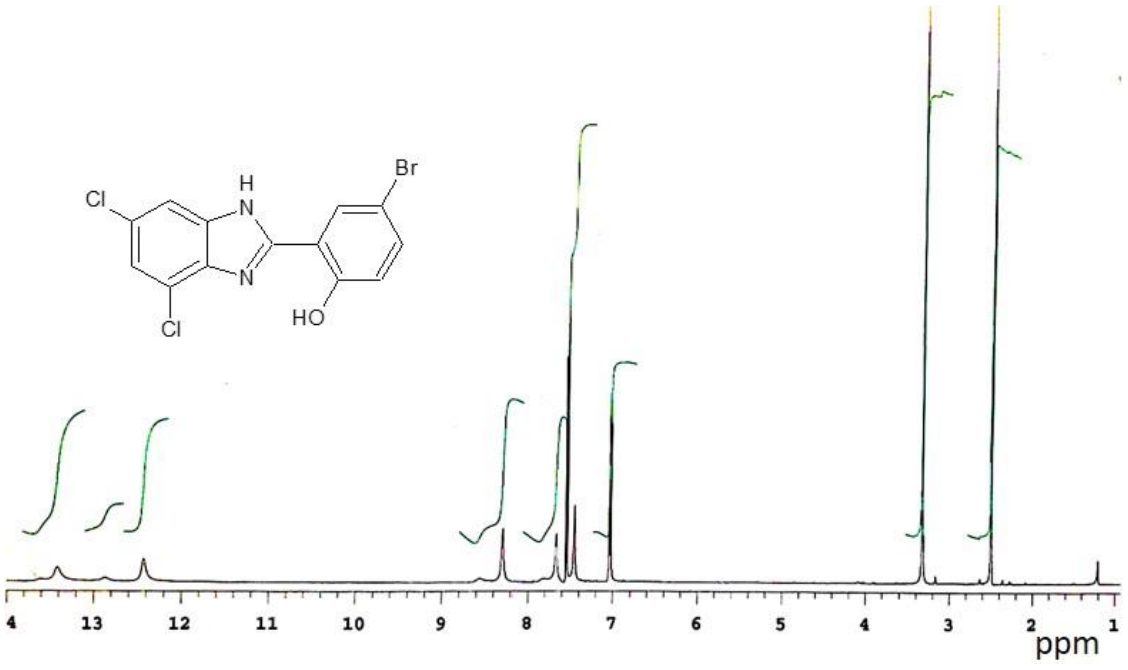

Fig. 3 – ^{1}H-NMR spectra of **HL$_2$** showing the isomeric structures.

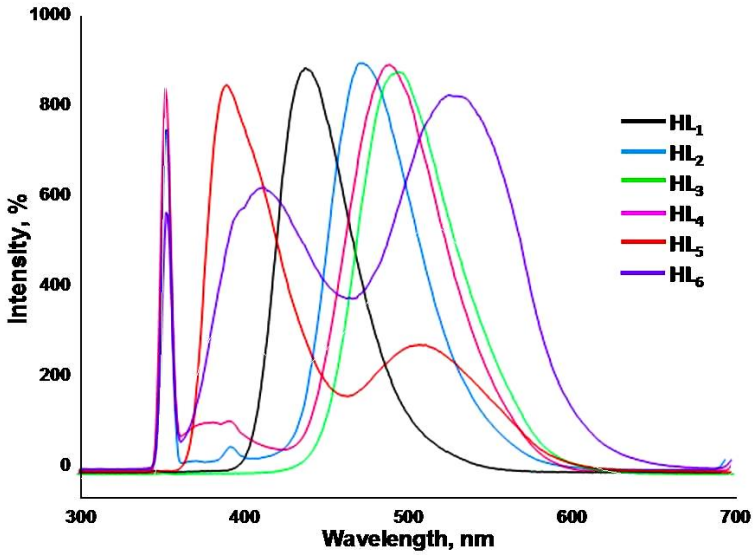

Fig. 4 – Fluorescence spectra of the ligands.

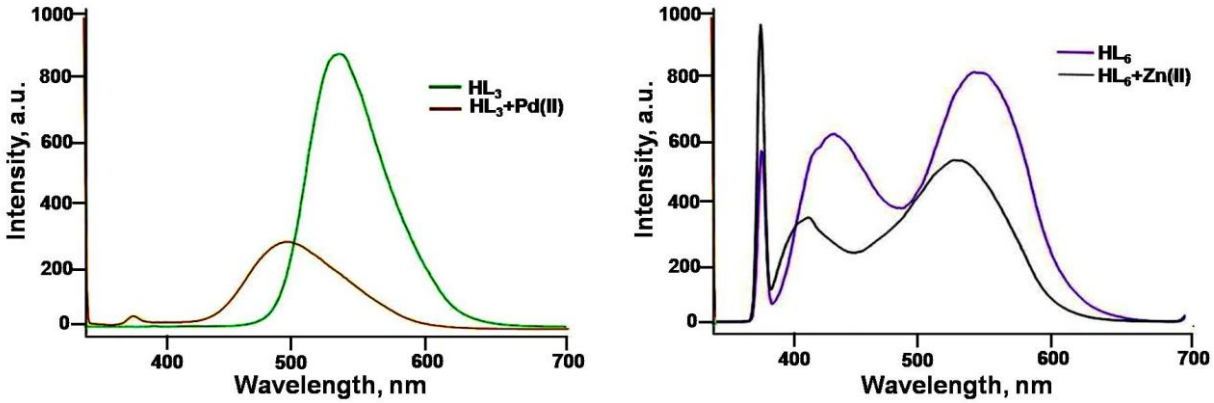

Fig. 5 – The comparative fluorescence spectra of **HL$_3$** and its Pd(II) complex (left) and **HL$_6$** and its Zn(II) complex (right).

In complex compounds, on the other hand, it was observed that the emission wavelengths move around to lower wavelength values while the fluorescence intensity decreases, in other words, there is a blue shift as expected. The comparative fluorescence spectra of **HL$_3$** with its Pd(II) complex and **HL$_6$** with its Zn(II) complex are shown in Figure 5. It was observed that **HL$_5$** and **HL$_6$** showed dual fluorescence properties. Considering that **HL$_5$** have broad medium and medium bands at 514 nm and 391 nm, respectively, it is possible to say that this ligand behaves differently from the others. Stronger intramolecular hydrogen bond formation and higher dissociation potential can be shown as the reason for this difference in this ligand, which also behaves differently in NMR.

It was reported that 2-(2'-hydroxyphenyl) benzimidazole (HPBI) and its derivatives can undergo an excited-state intramolecular proton transfer (ESIPT) from the acidic (hydroxyl proton) to the basic site (aromatic nitrogen) when photoexcitation changes their charge density distribution.[31-33] In the ground state, the enol form is usually the most stable form of HPBI. However, the most stable structure is usually the keto tautomer in the first excited singlet state. As a result, excitation of the enol form of benzimidazolylphenols tends to be followed by transformation to the keto form in the excited state *via* ESIPT reaction (Fig. 6).[33] The keto structure turned into the enol form as a consequence of complexation. And this change will affect the fluorescence characteristics of the complexes with respect to the ligands significantly. It is observed that all of the compounds have been emitting fluorescence in the visible region.

The presented experimental data suggests that the ligands form 4-coordinated (tetrahedral) complexes with $ZnCl_2$, $PdCl_2$ and $AuCl_3$, generally. The suggested structures for some complexes are represented in Figures 7–10.

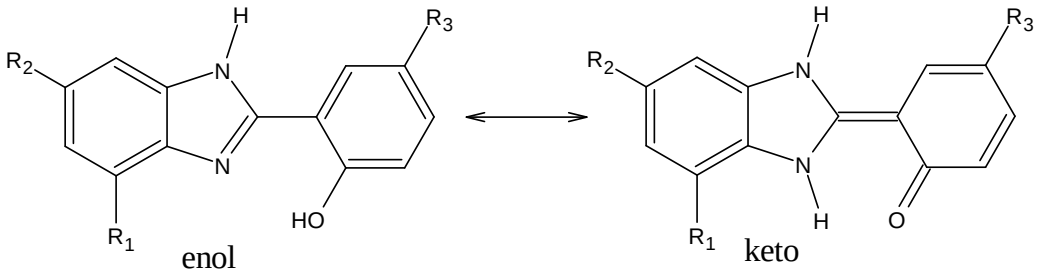

Fig. 6 – Enol-keto tautomerism in the ligands according to the ESIPT theory.

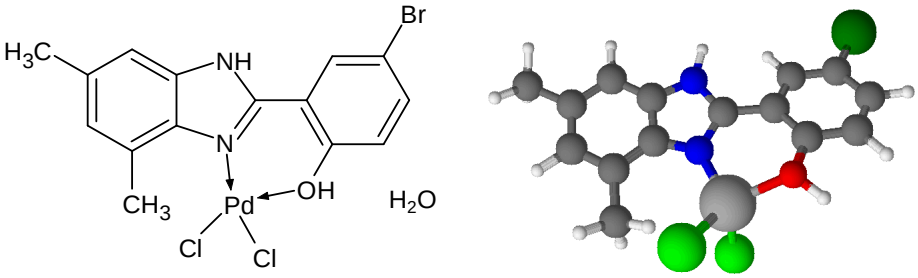

Fig. 7 – The suggested structure and ball-stick model for [Pd(**HL**$_1$)Cl_2]·H_2O complex.

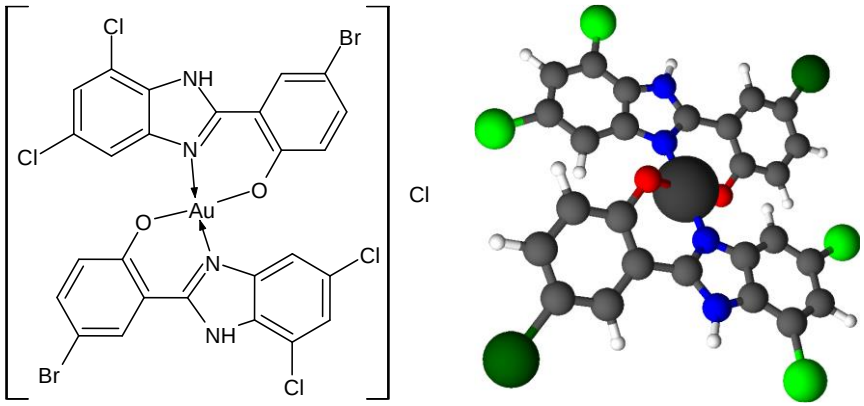

Fig. 8 – The suggested structure and ball-stick model for [Au(**L**$_2$)]Cl complex.

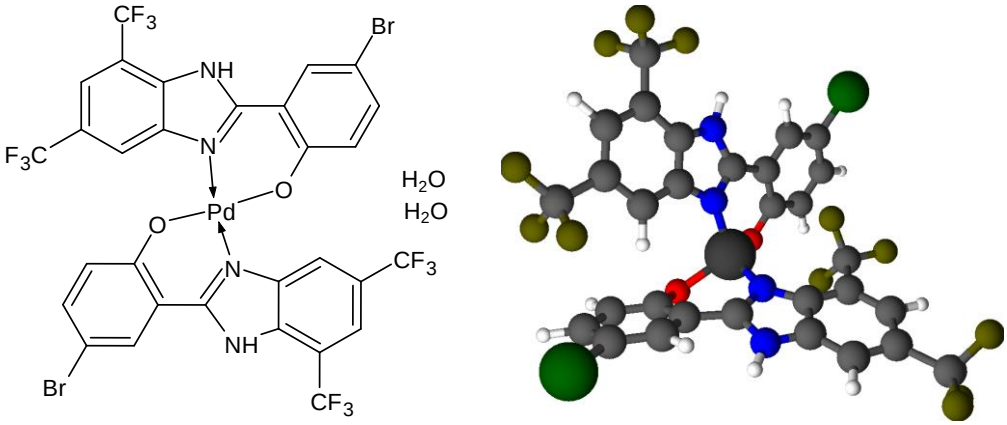

Fig. 9 – The suggested structure and ball-stick model for [Pd(**L**$_3$)$_2$]·$2H_2O$ complex.

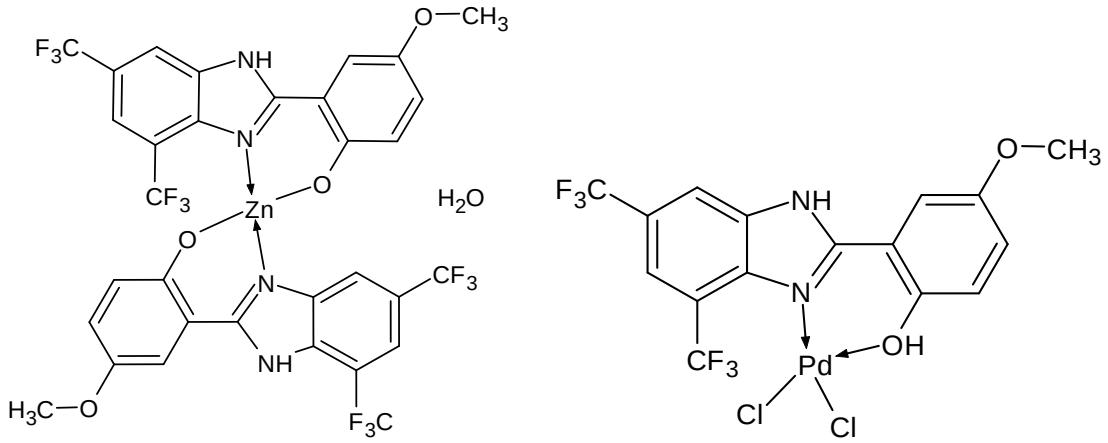

Fig. 10 – The suggested structures for [Pd(**HL$_6$**)Cl$_2$] and [Zn(**L$_6$**)$_2$]·H$_2$O complexes.

Table 1

In vitro antimicrobial activity of the compounds (MIC, μg/mL)

Compound	Microorganisms								
	Sa[*,a]	*Se*[a]	*Ec*[b]	*Kp*[b]	*Pa*[b]	*Pm*[b]	*Ca*	*Cp*	*Ct*
HL$_1$	-	-	-	-	-	-	-	-	-
HL$_2$	625	-	-	625	-	-	-	-	-
HL$_3$	-	-	-	-	-	-	-	-	-
HL$_4$	-	-	-	-	-	-	-	-	-
HL$_5$	-	-	-	-	-	-	-	-	-
HL$_6$	625	-	-	-	-	-	-	-	-
[Pd(**HL$_1$**)Cl$_2$]·H$_2$O	625	-	-	-	-	-	39.06	78.12	39.06
[Zn(**L$_1$**)$_2$]·4H$_2$O	625	-	-	-	625	-	625	-	-
[Au(**HL$_1$**)Cl$_2$]Cl·H$_2$O	78.12	39.06	78.12	39.06	78.12	39.06	39.06	78.12	78.12
[Pd(**L$_2$**)$_2$]·4H$_2$O	625	625	-	625	-	-	-	-	-
[Zn(**L$_2$**)$_2$]·4H$_2$O	-	-	-	-	-	-	-	-	-
[Au(**L$_2$**)$_2$]Cl·3H$_2$O·EtOH	9.76	9.76	19.53	9.76	19.53	4.88	156.25	156.25	39.06
[Pd(**L$_3$**)$_2$]·2H$_2$O	625	312.5	-	-	625	-	78.12	78.12	78.12
[Zn(**L$_3$**)$_2$]·2EtAc	-	625	-	-	-	-	-	-	-
[Au(**L$_3$**)(**HL$_3$**)Cl]Cl·4H$_2$O	4.88	4.88	19.53	19.53	39.06	4.88	-	-	-
[Pd(**HL$_4$**)$_2$Cl$_2$]·H$_2$O	625	-	-	625	625	625	-	-	-
[Zn(**HL$_4$**)$_2$Cl$_2$]·2H$_2$O	625	625	312.5	625	625	625	-	-	-
[Au(**HL$_4$**)$_2$Cl]Cl$_2$·4H$_2$O	39.06	19.53	78.12	19.53	78.12	39.06	19.53	39.06	39.06
[Pd(**HL$_5$**)(**L$_5$**)Cl]·2H$_2$O	625	625	312.5	-	625	625	625	625	625
[Zn(**L$_5$**)$_2$]·3H$_2$O	-	625	-	-	-	-	-	-	-
[Au(**HL$_5$**)Cl$_3$]·4H$_2$O	625	625	-	-	-	-	-	-	-
[Pd(**HL$_6$**)Cl$_2$]	-	-	-	-	-	-	-	-	-
[Zn(**L$_6$**)$_2$]·H$_2$O	-	-	-	-	-	-	-	-	-
[Au(**HL$_6$**)(**L$_6$**)Cl]Cl	39.06	78.12	78.12	156.25	78.12	156.25	156.25	312.5	312.5

Table 1 (continued)

$ZnCl_2$	-	-	-	-	-	-	625	312	625
$PdCl_2$	-	-	-	-	-	-	312	312	312
$AuCl_3$	19.5	39	9.75	9.75	39	9.75	156	156	156
References**	0.25	0.0625	0.0156	0.0078	1.0	0.0156	0.5	1.0	1.0

* *Sa Staphylococcus aureus* ATCC 6538 *Se Staphylococcus epidermidis* ATCC 12228
Ec Escherichia coli ATCC 8739 *Kp Klebsiella pneumoniae* ATCC 4352
Pa Pseudomonas aeruginosa ATCC 1539 *Pm Proteus mirabilis* ATCC 14153
Ca Candida albicans ATCC 10231 *Cp Candida parapsilosis* ATCC 22019
Ct Candida tropicalis ATCC 750
[a], Gram positive; [b], Gram negative
[c], - : No antimicrobial effect at 5000 μg/mL and lower dilutions
** Ciprofloxacin and Amphotericin B were used for bacteria and fungi, respectively.

Antimicrobial activity

The results concerning in vitro antimicrobial activity of the ligands and the complexes together with MIC values of compared the antibiotic and antifungal agents and the metal salts are presented in Table 1. It was observed that ligands were not active against microorganisms whereas the Pd(II) and Au(III) complexes show a remarkably high activity especially against fungi. $AuCl_3$ itself is also highly active against all microorganisms, considering its complexes with the **HL_1**, **HL_2**, **HL_4** and **HL_6**, it is possible to say that the activity against bacteria does not change much, but the activity against fungi appears to be increased.

It is noteworthy that the Au(III) complexes of **HL_1**, **HL_2**, **HL_4** and **HL_6** are effective against all microorganisms, and the $[Au(\mathbf{L_3})(\mathbf{HL_3})Cl]Cl{\cdot}4H_2O$ complex shows very high activity against bacteria only. It is observed that Au(III) complex of **HL_2** against *P. mirabilis* and Au(III) complex of **HL_3** against *S. aureus*, *S. epidermidis* and *P. mirabilis* have a superior activity such as MIC value of 4.88 μg/mL. Likewise, it is a remarkable observation that $[Zn(\mathbf{HL_4})_2Cl_2]{\cdot}2H_2O$ shows moderate activity against bacteria, while it is ineffective against fungi.

Similarly, the Pd(II) complexes of **HL_3** and **HL_5** show a wide spectrum of antimicrobial activity. It is interesting that the Pd(II) complexes of **HL_1** and **HL_3** are particularly active against fungi. Considering the moderate activity of $PdCl_2$ against fungi, it is possible to say that the activity in these compounds has increased.

EXPERIMENTAL

Chemistry and apparatus

All chemicals and solvents were of reagent grade and they were used without further purification.

Analytical data were obtained with a Thermo Finnigan Flash EA 1112 analyzer. Melting points were determined using a Buchi M-560 melting-point apparatus. Molar conductivity of the complexes was measured on a WTW Cond315i conductivity meter in DMF at 25 °C. NMR spectra were run on a Varian Unity Inova 500 NMR spectrometer. The residual DMSO-d_6 signal was also used as an internal reference. FT-IR spectra were recorded on a Bruker Optics Vertex 70 spectrometer using Attenuated Total Reflection (ATR) techniques between 400 and 4000 cm^{-1}. The Electron Spray Ionization-Mass Spectrometry (ESI-MS) analysis was carried out in positive ion modes using a Thermo Finnigan LCQ Advantage MAX LC/MS/MS in MeOH. Fluorescence spectra were performed on a Shimadzu RF-5301 PC Spectrofluorophotometer in EtOH (c = ~1×10^{-4} mol/L).

Synthesis of the ligands

Benzimidazole derivatives were prepared according to the literature procedure.[34,35] An appropriate aldehyde (3 mmol, *e.g.* 603 mg 5-bromosalicylaldehyde) and $NaHSO_3$ (3 mmol, 312.0 mg) were dissolved in ethanol+water mixture (20 mL + 2 mL) and stirred at room temperature ~3 h. Then appropriate *o*-phenylenediamine derivative (3 mmol, *e.g.* 531 mg of 4,6-dichloro-1,2-phenylenediamine) in 15 mL DMF was added to the reaction vessel and refluxed for 3 h. After cooling to the room temperature, the reaction mixture was poured into water (250 mL) and then a precipitate was formed. It was filtered, dried and crystallized from ethanol.

Synthesis of the complexes

One mmol of appropriate metal salt solutions (326 mg K_2PdCl_4 and 378 mg $KAuCl_4$ in 10 mL ethanol, and 136 mg anhydrous $ZnCl_2$ in 10 mL ethylacetate) was added gradually to a solution of the ligand (1 mmol, *e.g.* 317 mg of **HL_1**) in the solvent (15 mL) in the molar ratio 1:1, and heated to reflux for 3 hours. The resulting precipitates were filtered off, washed with a very small amount of methanol and kept in desiccator over anhydrous calcium chloride to dry.

4-Bromo-2-(4,6-dimethyl-1H-benzimidazol-2-yl)phenol (HL₁): Yield: 76%. Slightly yellow solid. M.p.: 211 °C. Calcd. for $C_{15}H_{13}BrN_2O$ (%): C, 56.80; H, 4.13; N, 8.83. Found (%): C, 56.45; H, 3.93; N, 8.97. MW: 317.18 g/mol. ESI-MS, m/z (%): 317.24 (100), 319.26 (98.2), 320.28 (14.4). FT-IR spectroscopy (ATR, cm^{-1}): 3261 m,br ν(OH+NH), 3064 m ν(CH_{arom}), 2920 m ν(CH_{aliph}), 1633 m ν(C=N), 1615

m ν(C=C), 1587 m, 1485 s, 1376 m, 1257 s ν(C–O), 1088 m, 841 m, 810 s δ(CH_{arom}), 714 m, 597 m, 550 m, 423 m. ^{1}H-NMR spectroscopy (500 MHz, ppm, isomeric ratio 2:3): 13.57 s,br (0.4H, NH), 13.47 s,br (0.6H, OH), 13.08 s (0.6H, NH), 12.85 s (0.4H, OH), 8.44 s (0.4H, H7), 8.25 s (0.6H, H7), 7.49 dd (1H, J=8.8, 2.4, H5'), 7.33 s (0.4H, H5), 7.21 s (0.6H, H5), 6.99 d (1H, J=8.8, H6'), 6.93 s (1H, H3'), 2.42 s (6H, 2×CH_3). Fluorescence spectroscopy (λ, nm): 459 s.

[Zn(L$_1$)$_2$]·4H$_2$O: Light brown solid, yield: 72%. M.p.> 300 °C. Calcd. for $C_{30}H_{32}Br_2N_4O_6Zn$ (%): C, 46.81; H, 4.19; N, 7.28. Found (%): C, 46.03; H, 4.06; N, 7.76. MW: 769.80 g/mol. Molar conductivity: 24.0 $\Omega^{-1}cm^2mol^{-1}$. FT-IR spectroscopy (ATR, cm^{-1}): 3206 m,br ν(OH+NH), 3062 m ν(CH_{arom}), 2917 m ν(CH_{aliph}), 1633 m ν(C=N), 1605 m ν(C=C), 1549 m, 1485 s, 1371 m, 1249 m ν(C–O), 1225 s, 1136 m, 1095 m, 842 m, 815 s δ(CH_{arom}), 752 m, 712 m, 651 m, 571 m, 521 m, 428 m. ^{1}H-NMR spectroscopy (500 MHz, ppm): 13.20 s,br (1H, NH), 8.32 s (1H, H7), 7.48 d (1H, J=8.7, H5'), 7.25 s (1H, H5), 6.99 d (1H, J=8.7), 6.93 s (1H, H3'), 2.42 s (6H, 2×CH_3). Fluorescence spectroscopy (λ, nm): 423 m, 447 sh.

[Pd(HL$_1$)Cl$_2$]·H$_2$O: Light brown solid, yield: 65%. M.p.>300 °C. Calcd. for $C_{15}H_{15}BrCl_2N_2O_2Pd$ (%): C, 35.15; H, 2.95; 5.47. Found (%): C, 35.03; H, 3.21; N, 4.77. MW: 512.5 g/mol. Molar conductivity: 25.0 $\Omega^{-1}cm^2mol^{-1}$. FT-IR spectroscopy (ATR, cm^{-1}): 3290 m ν(OH+NH), 3094 m ν(CH_{arom}), 2946 m ν(CH_{aliph}), 1634 m ν(C=N), 1600 m ν(C=C), 1513 m, 1447 m, 1368 m, 1272 s ν(C–O), 1190 m, 1108 s, 968 m, 899 m, 820 m δ(CH_{arom}), 748 m, 671 m, 545 m, 465 m, 415 m. ^{1}H-NMR spectroscopy (500 MHz, ppm, isomer, ratio: 2:3): 13.57 s,br (NH, 0.4H), 13.47 s,br (OH, 0.6H), 13.08 s (NH, 0.6H), 12.85 s (OH, 0.4H), 8.44 s (H7, 0.4H), 8.25 s (H7, 0.6H), 7.49 dd (1H, J=8.8, 2.4, H4'), 7.33 s (H5, 0.4H), 7.21 s (H5, 0.6H), 6.99 d (1H, J=8.8 H3'), 6.93 s (1H, H6'), 2.42 s (6H, 2×CH_3). Fluorescence spectroscopy (λ, nm): 499 m.

[Au(HL$_1$)Cl$_2$]Cl·H$_2$O: Dark orange solid. Yield: 64%. M.p.: 286 °C. Calcd. for $C_{15}H_{15}AuBrCl_3N_2O_2$ (%): C, 28.22; H, 2.37; N, 4.39. Found (%): C, 26.95; H, 2.09; N, 4.12. MW: 638.5 g/mol. Molar conductivity: 65.0 $\Omega^{-1}cm^2mol^{-1}$. FT-IR spectroscopy (ATR, cm^{-1}): 3242 m ν(OH+NH), 3065 m ν(CH_{arom}), 2925 m ν(CH_{aliph}), 1632 m ν(C=N), 1605 m ν(C=C), 1558 m, 1495 m, 1386 m, 1239 s ν(C–O), 1140 m, 1094 s, 856 m, 821 m δ(CH_{arom}), 737 m, 626 m, 593 m, 500 m, 460 m. ^{1}H-NMR spectroscopy (500 MHz, ppm): 13.41 s,br (1H, NH), 8.31 s,br (1H, H7), 7.53 d,br (1H, J=9.3, H5'), 7.28 s (1H, H5), 7.10 d (1H, J=8.8), 6.97 s (1H, H3'), 2.41 s (6H, 2×CH_3). Fluorescence spectroscopy (λ, nm): 423 m, 447 sh.

4-Bromo-2-(4,6-dichloro-1H-benzimidazol-2-yl)phenol (HL$_2$): Slightly yellow solid, yield: 71%. M.p.: 275 °C. Calcd. for $C_{13}H_7BrCl_2N_2O$ (%): C, 43.61; H, 1.97; N, 7.82. Found (%): C, 43.46; H, 1.82; N, 7.67. MW: 358.02 g/mol. ESI-MS, m/z (%): 359.2 (100), 357.2 (63.4), 361.2 (47.4). FT-IR spectroscopy (ATR, cm^{-1}): 3296 m,br ν(OH+NH), 3099 m ν($CH_{arom.}$), 2965 m ν($CH_{aliph.}$), 1626 m ν(C=N), 1577 m ν(C=C), 1480 s, 1373 m, 1249 s ν(C–O), 1197 m, 966 m, 844 m, 812 s δ(CH_{arom}), 627 m, 572 m, 542 m, 415 m. ^{1}H-NMR spectroscopy (500 MHz, ppm, isomeric 1:9): 13.61 s,br (0.1H, NH), 13.41 s,br (0.9H, NH), 12.87 s,br (0.1H, OH), 12.43 s (0.9H, OH), 8.56 s,br (0.1H, H5), 8.30 s (0.9H, H5), 7.81 s,br (0.1H, H7), 7.64 s (0.9H, H7), 7.55 dd (1H, J=8.8, 2.9, H5'), 7.45 s (1H, H3'), 7.03 d (1H, J=8.8, H6'). Fluorescence spectroscopy (λ, nm): 475 s.

[Zn(L$_2$)$_2$]·4H$_2$O: Dark grey solid, yield: 72%. M.p.: 307 °C. Calcd. for $C_{26}H_{20}Br_2Cl_4N_4O_6Zn$ (%): C, 36.67; H, 2.37; N, 6.58. Found (%): C, 36.28; H, 2.53; N, 6.33. MW: 851.47 g/mol. Molar conductivity: 18.0 $\Omega^{-1}cm^2mol^{-1}$. FT-IR spectroscopy (ATR, cm^{-1}): 3174 m,br ν(OH+NH), 3052 m ν(CH_{arom}), 2962 m ν(CH_{aliph}), 1622 m ν(C=N), 1609 m ν(C=C), 1543 m, 1484 s, 1419 m, 1238 m ν(C–O), 1190 m, 1091 m, 985 m, 847 m, 812 s δ(CH_{arom}), 712 m, 643 m, 540 m, 421 m. ^{1}H-NMR spectroscopy (500 MHz, ppm, isomeric ratio 2:8): 13.60 s,br (0.2H, NH), 13.40 s,br (0.8H, NH), 8.58 s,br (0.2H, H5), 8.27 s (0.8H, H5), 7.79 s,br (0.2H, H7), 7.64 s (0.8H, H7), 7.53 dd (1H, J=8.7, 2.5, H5'), 7.42 s (1H, H3'), 7.02 d (1H, J=8.7, H6'). Fluorescence spectroscopy (λ, nm): 422 sh, 472 m,br.

[Pd(L$_2$)$_2$]·4H$_2$O: Dark grey solid, yield: 73%. M.p.:>300 °C. Calcd. for $C_{26}H_{16}Br_2Cl_4N_4O_4Pd$ (%): C, 36.46; H, 1.88; N, 6.54. Found (%): C, 35.80; H, 1.65; N, 6.31. MW: 856.47 g/mol. Molar conductivity: 29.0 $\Omega^{-1}cm^2mol^{-1}$. FT-IR spectroscopy (ATR, cm^{-1}): 3282 m,br ν(OH+NH), 3165 m,br ν(CH_{arom}), 2937 m,br ν(CH_{aliph}), 1630 m ν(C=N), 1609 m ν(C=C), 1537 m, 1474 m, 1368 m, 1275 s ν(C–O), 1201 m, 1124 m, 1016 m, 968 m, 889 m, 825 m δ(CH_{arom}), 696 m, 650 m, 621 m, 539 m, 409 m. ^{1}H-NMR spectroscopy (500 MHz, ppm): 13.75 s,br (1H, NH), 8.40 s (1H, H5), 8.29 s (1H, H7), 7.87 s (1H, H3'), 7.61 dd (1H, J=8.8, 2.4, H5'), 7.09 d (1H, J=8.8 Hz, H6'). Fluorescence spectroscopy (λ, nm): 482 m,br.

[Au(L$_2$)$_2$]Cl·3H$_2$O·EtOH: Brown solid, yield: 68%. M.p.: 253 °C. Calcd. for $C_{28}H_{24}Br_2Cl_5N_4O_6Au$ (%): C, 32.13; H, 2.31; N, 5.35. Found (%): C, 32.02; H, 2.68; N, 5.14. MW: 1046.55 g/mol. Molar conductivity: 68.0 $\Omega^{-1}cm^2mol^{-1}$. FT-IR spectroscopy (ATR, cm^{-1}): 3215 m,br ν(OH+NH), 3074 m ν(CH_{arom}), 2917 m ν(CH_{aliph}), 1642 m ν(C=N), 1608 m ν(C=C), 1487 m, 1357 m, 1277 m ν(C–O), 1191 m, 1110 s, 986 m, 882 m, 825 m δ(CH_{arom}),737 m, 652 m, 628 m, 535 m. ^{1}H-NMR spectroscopy (500 MHz, ppm): 8.37 s,br (1H, H5), 8.31 s,br (1H, H7), 7.81 s,br (1H, H3'), 7.54 s,br (1H, H5'), 7.04 s,br (1H, H6'). Fluorescence spectroscopy (λ, nm): 482 m,br.

2-[4,6-Bis(trifluoromethyl)-1H-benzimidazol-2-il]-4-bromofenol (HL$_3$): Beige solid, yield: 78%. M.p.: 128 °C. Calcd. for $C_{15}H_7BrF_6N_2O$ (%): C, 42.38; H, 1.66; N, 6.59. Found (%): C, 42.51; H, 1.80; N, 6.44. MW: 425.12 g/mol. ESI-MS, m/z (%): 423.8 (100), 425.5 (99.6), 426.5 (12.5). FT-IR spectroscopy (ATR, cm^{-1}): 3383 m,br ν(OH+NH), 3073 m ν($CH_{arom.}$), 2972 m ν($CH_{aliph.}$), 1623 m ν(C=N), 1609 m ν(C=C), 1486 m, 1359 m, 1276 m ν(C–O), 1151 m, 1109 s, 944 m, 831 m δ(CH_{arom}), 652 m, 550 m, 410 m. ^{1}H-NMR spectroscopy (500 MHz, ppm, isomeric ratio 3:2): 13.67 s,br (1H, NH), 12.29 s,br (1H, OH), 8.39 s,br (1H, H5), 7.87 s (1H, H7), 7.62 dd (1H, J=8.8, 2.4, H5'), 7.57 d (1H, J=2.4, H3'), 6.96 d (1H, J=8.8, H6'). Fluorescence spectroscopy (λ, nm): 495 m.

[Zn(L$_3$)$_2$]·2EtOAc: Dark grey solid, yield: 75%. M.p.: 238 °C. Calcd. for $C_{36}H_{24}Br_2F_{12}N_4O_6Zn$ (%):C, 40.72; H, 2.28; N, 5.28. Found (%): C, 40.95; H, 2.61; N, 5.55. MW: 1061.78 g/mol. Molar conductivity: 12.0 $\Omega^{-1}cm^2mol^{-1}$. FT-IR spectroscopy (ATR, cm^{-1}): 3224 m,br ν(OH+NH), 3081 m ν(CH_{arom}), 2935 m,br ν(CH_{aliph}), 1625 m ν(C=N), 1588 m ν(C=C), 1485 m, 1358 m, 1278 m ν(C–O), 1246 m, 1201 m, 1112 s, 978 m, 883 m, 828 m δ(CH_{arom}), 731 m, 651 m, 630 m, 535 m, 404 m. ^{1}H-NMR spectroscopy (500 MHz,

ppm): 13.65 s,br (NH), 12.25 s,br (OH), 8.36 s (1H, H5), 8.26 s (1H, H7), 7.84 s (1H, H3'), 7.58 dd (1H, J=8.7, 2.5, H5'), 7.06 d (1H, J=8.7, H6'). Fluorescence spectroscopy (λ, nm): 428 m,br, 485 m.

[Pd(L$_3$)$_2$]·2H$_2$O: Dark grey solid, yield: 74%. M.p.: 328 °C. Calcd. for $C_{30}H_{16}Br_2F_{12}N_4O_4Pd$ (%): C, 36.37; H, 1.63; N, 5.66. Found (%): C, 35.80; H, 1.78; N, 5.34. MW: 990.68 g/mol. Molar conductivity: 36.0 $\Omega^{-1}cm^2mol^{-1}$. FT-IR spectroscopy (ATR, cm^{-1}): 3263 m,br ν(OH+NH), 3059 m ν(CH_{arom}), 2974 m ν($CH_{aliph.}$), 1618 m ν(C=N), 1602 m ν(C=C), 1585 m, 1477 m, 1448 m, 1334 m, 1287 m ν(C–O), 1242 m, 1109 m, 993 m, 841 m, 818 s δ(CH_{arom}), 629 m, 596 m, 498 m. ^{1}H-NMR spectroscopy (500 MHz, ppm): 13.18 s (NH), 9.19 d (1H, J=2.44 Hz, H3'), 7.78 d (1H, J=2.44, 8.80 Hz, H5'), 7.76 s (1H, H7), 7.15 d (1H, J=8.8, H6'), 6.98 s (1H, H5). Fluorescence spectroscopy (λ, nm): 457 m.

[Au(L$_3$)(HL$_3$)Cl]Cl·4H$_2$O: Dark grey solid, yield: 67%. M.p.: 271 °C. Calcd. for $C_{30}H_{22}Br_2Cl_3F_{12}N_4O_6Au$ (%): C, 29.40; H, 1.81; N, 4.57. Found (%): C, 28.84; H, 1.68; N, 4.46. MW: 1225.63 g/mol. Molar conductivity: 91.0 $\Omega^{-1}cm^2mol^{-1}$. FT-IR spectroscopy (ATR, cm^{-1}): 3306 m,br ν(OH+NH), 3078 m ν($CH_{arom.}$), 2983 m ν($CH_{aliph.}$), 1641 m ν(C=N), 1611 m ν(C=C), 1488 m, 1360 m, 1279 m ν(C–O), 1198 m, 1131 s, 987 m, 891 m, 824 m δ(CH_{arom}), 732 m, 655 m, 630 m, 537 m, 465 m. ^{1}H-NMR spectroscopy (500 MHz, ppm): 8.39 s,br (1H, H5), 8.24 s (1H, H7), 7.80 s (1H, H6'), 7.54 dd (1H, J=8.8, 2.4, H3'), 7.05 dd (1H, J=8.8, 2.0, H5'). Fluorescence spectroscopy (λ, nm): 493 m.

2-(4,6-Dimethyl-1H-benzimidazol-2-yl)-4-methoxyphenol (HL$_4$): Light yellow solid, yield: 78%. M.p.: 186 °C. Calcd. for $C_{16}H_{16}N_2O_2$ (%): C, 71.62; H, 6.01; N, 10.44. Found (%): C, 71.45; H, 6.12; N, 10.27. MW: 268.31 g/mol. ESI-MS, m/z (%): 269.3 (100), 270.3 (17.0). FT-IR spectroscopy (ATR, cm^{-1}): 3263 m,br ν(OH+NH), 3057 m ν(CH_{arom}), 2919 m ν(CH_{aliph}), 2832 m, 1636 m ν(C=N), 1596 m ν(C=C), 1503 s, 1392 m, 1268 m ν(C–O), 1220 s, 1048 m, 831 m, 800 s δ(CH_{arom}), 706 m, 600 m, 579 m, 521 m, 408 m. ^{1}H-NMR spectroscopy (ppm, isomeric ratio 3:2): 12.95 s,br (0.6H, NH+OH), 12.80 s,br (0.4H, NH+OH), 7.75 s,br (0.4H, H7), 7.65 s,br (0.6H, H5), 7.30 s,br (0.4H, H5), 7.22 s,br (0.6H, H7), 6.97 dd (1H, J=8.8, 2.9, H5'), 6.93 s (1H, H3'), 6.91 d (1H, J=8.8, H6'), 3.81 s (3H, OCH_3), 2.53 s (3H, CH_3), 2.41 s (3H, CH_3). Fluorescence spectroscopy (λ, nm): 489 s.

[Zn(HL$_4$)$_2$Cl$_2$]·2H$_2$O: Dark grey solid, yield: 74%. M.p.: 284 °C. Calcd. for $C_{32}H_{36}Cl_2N_4O_6Zn$ (%): C, 54.21; H, 5.12; N, 7.90. Found (%): C, 53.88; H, 4.87; N, 7.65. MW: 708.95 g/mol. Molar conductivity: 28.0 $\Omega^{-1}cm^2mol^{-1}$. FT-IR spectroscopy (ATR, cm^{-1}): 3327 m ν(OH+NH), 3220 m, 3082 m,br ν(CH_{arom}), 2970 m ν(CH_{aliph}), 1628 m ν(C=N), 1559 m ν(C=C), 1498 s, 1452 m, 1295 m, 1224 mν(C–O), 1189 m, 1040 m, 843 m, 813 m δ(CH_{arom}),784 m, 645 m, 603 m, 584 m, 521 m, 485 m, 414 m. ^{1}H-NMR spectroscopy (500 MHz, ppm): 12.94 s (1H, NH), 12.75 s,br (1H, OH), 7.66 s,br, (1H, H7), 7.23 s,br (1H, H5), 6.95 s,br (1H, H3'), 6.90 (1H, H6'), 6.54 m,br (1H, H5'), 3.79 s (3H, OCH_3), 2.54 s (3H, CH_3), 2.39 s (3H, CH_3). Fluorescence spectroscopy (λ, nm): 490 m.

[Pd(HL$_4$)$_2$Cl$_2$]·H$_2$O: Dark grey solid, yield: 70%. M.p.: 261 °C. Calcd. for $C_{32}H_{34}Cl_2N_4O_5Pd$ (%): C, 52.51; H, 4.68; N, 7.65. Found (%): C, 52.52; H, 4.38; N, 7.48. MW: 731.96 g/mol. Molar conductivity: 42.0 $\Omega^{-1}cm^2mol^{-1}$. FT-IR spectroscopy (ATR, cm^{-1}): 3298 m ν(NH), 3070 m,br ν(CH_{arom}), 2990 m ν($CH_{aliph.}$), 2918 m, 1621 m ν(C=N), 1602 m ν(C=C), 1487 s, 1450 m, 1350 m, 1215 m, 1190 s ν(C–O), 1032 m, 848 m, 817 m δ(CH_{arom}), 781 m, 655 m, 580 m, 523 m, 489 m. ^{1}H-NMR spectroscopy (500 MHz, ppm): 13.09 s (NH), 9.88 s (1H, OH), 8.88 s (1H, H5), 7.86 s (1H, H7), 7.23 dd (1H, J= 8.8, 2.4, H5'), 7.11 d (1H, J=8.8, H6'), 6.98 s (1H, H3'), 3.83 s (3H, OCH_3), 2.46 s (6H, 2×CH_3). Fluorescence spectroscopy (λ, nm): 480 m.

[Au(HL$_4$)$_2$Cl]Cl$_2$·4H$_2$O: Brown solid, yield: 60%. M.p.: 211 °C. Calcd. for $C_{32}H_{40}Cl_3N_4O_8Au$ (%): C, 42.14; H, 4.42; N, 6.14. Found (%): C, 42.46; H, 4.71; N, 5.83. MW: 912.01 g/mol. Molar conductivity: 106.0 $\Omega^{-1}cm^2mol^{-1}$. FT-IR spectroscopy (ATR, cm^{-1}): 3198 m,br ν(OH+NH), 3061 m ν(CH_{arom}), 2973 m ν(CH_{aliph}), 2920 m, 2840 m, 1736 m ν(C=N), 1631 m ν(C=C), 1564 m, 1505 s, 1456 m, 1385 s, 1253 m ν(C–O), 1129 m, 1034 m, 845 m, 821 m δ(CH_{arom}), 751 m, 683 m, 592 m, 503 m, 477 m. ^{1}H-NMR spectroscopy (500 MHz, ppm): 7.77 s,br (1H, H7), 7.37 s,br, (1H, H5), 7.08 s,br (1H, H5'), 6.90 s,br (1H, H3'), 6.54 s,br (1H, H6'), 3.73 s,br (3H, OCH_3), 2.29 s,br (6H, 2×CH_3). Fluorescence spectroscopy (λ, nm): 493 m.

2-(4,6-Dichloro-1H-benzimidazol-2-yl)-4-methoxyphenol (HL$_5$): Light yellow solid, yield: 81%. M.p.: 269 °C. Calcd. for $C_{14}H_{10}Cl_2N_2O_2$ (%): C, 54.39; H, 3.26; N, 9.06. Found (%): C, 54.22; H, 3.15; N, 9.17. MW: 309.15 g/mol. ESI-MS, m/z (%): 307.2 (100), 309.3 (50.3), 311.4 (21.4). FT-IR spectroscopy (ATR, cm^{-1}): 3234 m,br ν(OH+NH), 3078 m ν(CH_{arom}), 2927 m ν($CH_{aliph.}$), 1640 m ν(C=N), 1601 m ν(C=C), 1580 m, 1501 s, 1373 m, 1292 m, 1252 m ν(C–O), 1225 s, 1074 m, 991 m, 843 m, 754 s δ(CH_{arom}), 685 m, 593 m, 544 m, 419 m. ^{1}H-NMR spectroscopy (500 MHz, ppm): 7.70 s,br (1H, H5), 7.68 s,br (1H, H7), 7.45 d (1H, J=1.5, H3'), 7.03 dd (1H, J=8.8, 2.9, H5'), 6.99 d (1H, J=8.8, H6'), 3.80 s (3H, OCH_3). Fluorescence spectroscopy (λ, nm): 391 m, 511 m,br.

[Zn(L$_5$)$_2$]·3H$_2$O: Dark yellow solid, yield: 73%. M.p.: 211 °C. Calcd. for $C_{28}H_{24}Cl_4N_4O_7Zn$ (%): C, 45.71; H, 3.29; N, 7.62. Found (%): C, 45.92; H, 3.17; N, 7.61. MW: 735.71 g/mol. Molar conductivity: 21.0 $\Omega^{-1}cm^2mol^{-1}$. FT-IR spectroscopy (ATR, cm^{-1}): 3244 m,br ν(OH+NH), 3089 m ν(CH_{arom}), 2976 m ν(CH_{aliph}), 1604 m ν(C=N), 1580 m ν(C=C), 1500 s, 1401 m, 1322 m, 1228s ν(C–O), 1084 m, 976 m, 842 m, 814 m, δ(CH_{arom}),765 m, 634 m, 584 m, 425 m. ^{1}H-NMR spectroscopy (500 MHz, ppm): 7.72 s,br (1H, H5), 7.69 s,br (1H, H7), 7.47 d (1H, J=2.0 Hz, H3'), 7.04 dd (1H, J=9.3, 8.8, 2.9, 2.4, H5'), 7.00 d (1H, J=8.8, H6'), 3.81 s (3H, OCH_3). Fluorescence spectroscopy (λ, nm): 392 m,br, 515 m.

[Pd(HL$_5$)(L$_5$)Cl]·2H$_2$O: Dark grey solid, yield: 77%. M.p.: 293 °C. Calcd. for $C_{28}H_{23}Cl_5N_4O_6Pd$ (%): C, 42.29; H, 2.92; N, 7.05. Found: (%): C, 41.62; H, 2.43; N, 6.72. MW: 795.19 g/mol. Molar conductivity: 27.0 $\Omega^{-1}cm^2mol^{-1}$. FT-IR spectroscopy (ATR, cm^{-1}): 3392 m,br ν(OH), 3196 m ν(NH), 3078 m ν(CH_{arom}), 2960 m ν($CH_{aliph.}$), 2840 m, 1626 m ν(C=N), 1605 m ν(C=C), 1583 m, 1538 m, 1501 s, 1441 m, 1332 m, 1246 m, ν(C–O), 1220 m, 1161 m, 1077 m, 1032 m, 984 m, 861 s δ(CH_{arom}), 813 m, 676 m, 568 m, 537 m, 483 m, 414 m. ^{1}H-NMR spectroscopy (500 MHz, ppm): 8.67 d (1H, J=2.9, H5), 8.03 d (1H, J=1.5, H7), 7.70 d,br (1H, J=8.8 Hz, H3'), 7.62 s (1H, H6'), 7.29 dd (1H, J=8.8, 2.9 Hz, H4'), 3.84 s (3H, OCH_3). Fluorescence spectroscopy (λ, nm): 393 m, 466 w.

[Au(HL5)Cl3]·4H2O: Brown solid, yield: 63%. M.p: 216 °C. Calcd. for $C_{14}H_{18}Cl_5N_2O_6Au$ (%): C, 24.56; H, 2.65; N, 4.09. Found (%): C, 23.70; H, 2.30; N, 2.85. MW: 684.53 g/mol. Molar conductivity: 42.0 $\Omega^{-1}cm^2mol^{-1}$. FT-IR spectroscopy (ATR, cm^{-1}): 3296 m,br ν(OH+NH), 3078 m ν(CH_{arom}), 2920 m ν($CH_{aliph.}$), 1733 m ν(C=N), 1611 m ν(C=C), 1558 m, 1507 m, 1460 m, 1391 m, 1242 m ν(C–O), 1223 s, 1078 m, 1034 m, 994 m, 855 m, 813 m δ(CH_{arom}), 789 m, 671 m, 664 m, 590 m, 529 m, 409 m. ^{1}H-NMR spectroscopy (500 MHz, ppm): 7.95 s,br (1H, H5), 7.79 br (1H, H7), 7.56 d,br (1H, J=4.9, H3'), 7.12 s,br (1H, H5'), 7.07 d,br (1H, J=6.8, H6'), 3.82 s (3H, OCH_3). Fluorescence spectroscopy (λ, nm): 391 m,br, 508 m,br.

2-[4,6-Bis(trifluoromethyl)-1H-benzimidazol-2-yl]-4-methoxyphenol (HL6): Cream color solid, yield: 81%. M.p.: 157 °C. Calcd. for $C_{16}H_{10}F_6N_2O_2$ (%): C, 51.07; H, 2.68; N, 7.45. Found (%): C, 50.93; H, 2.79; N, 7.61. MW: 376.25 g/mol. ESI-MS, m/z (%): 379.1 (100), 377.1 (77.4), 380.2 (14.5). FT-IR spectroscopy (ATR, cm^{-1}): 3234 m,br ν(OH+NH), 3077 m ν(CH_{arom}), 2925 m ν($CH_{aliph.}$), 1612 m ν(C=N), 1601 m ν(C=C), 1580 m, 1503 s, 1374 m, 1268 m ν(C–O), 1226 s, 1188 m, 1074 m, 844 m, 754 s δ(CH_{arom}), 685 m, 593 m, 545 m, 418 m. ^{1}H-NMR spectroscopy (500 MHz, ppm): 13.38 s (1H, NH), 11.90 s (1H, OH), 7.66 s,br (2H, H5+H7), 7.45 s,br (1H, H3'), 7.04 dd (1H, J=8.8, 2.9, H5'), 6.99 d (1H, J=8.8, H6'), 3.81 s (3H, OCH_3). Fluorescence spectroscopy (λ, nm): 411 m,br, 531 m,br.

[Zn(L6)2]·H2O: Dark yellow solid, yield: 71%. M.p.: 261 °C. Calcd. for $C_{32}H_{20}F_{12}N_4O_5Zn$ (%): C, 46.09; H, 2.42; N, 6.72. Found (%): C, 46.14; H, 2.67; N, 6.98. MW: 833.89 g/mol. Molar conductivity: 27.0 $\Omega^{-1}cm^2mol^{-1}$. FT-IR spectroscopy (ATR, cm^{-1}): 3230 m,br ν(OH+NH), 3087 m ν(CH_{arom}), 2976 m ν(CH_{aliph}), 1631 m ν(C=N), 1605 m ν(C=C), 1580 m, 1503 s, 1401 m, 1228 s ν(C–O), 1085 m, 1031 m, 978 m, 846 m, 813 m δ(CH_{arom}), 714 m, 633 m, 585 m, 426 m, 411 m. ^{1}H-NMR spectroscopy (500 MHz, ppm): 7.72 s,br (1H, H7), 7.70 s,br (1H, H5), 7.47 d (1H, J=1.9, H3'), 7.4 dd (1H, J=9.3, 2.9, H5'), 7.00 d (1H, J=9.3, H6'), 3.81 s (3H, OCH_3). Fluorescence spectroscopy (λ, nm): 391 m,br, 514 m.

[Pd(HL6)Cl2]: Dark grey solid, yield: 67%. M.p.: >300 °C. Calcd. for $C_{16}H_{10}Cl_2F_6N_2O_2Pd$ (%): C, 34.71; H, 1.82; N, 5.06. Found (%): C, 34.52; H, 2.26; N, 5.36. MW: 553.58 g/mol. Molar conductivity: 19.0 $\Omega^{-1}cm^2mol^{-1}$. FT-IR spectroscopy (ATR, cm^{-1}): 3235 m,br ν(OH+NH), 3035 m ν(CH_{arom}), 2939 m ν($CH_{aliph.}$), 1591 m ν(C=N), 1519 m ν(C=C), 1456 m, 1337 m, 1208 m ν(C–O), 1119 s, 1024 m, 968 m, 822 m δ(CH_{arom}), 731 m, 675 m, 551 m, 465 m, 412 m. ^{1}H-NMR spectroscopy (500 MHz, ppm): 13.38 s (1H, NH), 11.90 s (1H, OH), 7.66 s,br (2H, H5+H7), 7.45 s,br (1H, H3'), 7.04 dd (1H, J=8.8, 2.9, H5'), 6.99 d (1H, J=8.8, H6'), 3.81 s (3H, OCH_3). Fluorescence spectroscopy (λ, nm): 392 m,br, 511 m.

[Au(HL6)(L6)Cl]Cl·5H2O·EtOH: Brownish-red solid. Yield: 63%. M.p.: 198 °C. Calcd. for $C_{34}H_{35}Cl_2F_{12}N_4O_{10}Au$ (%): C, 35.34; H, 3.05; N, 4.85. Found (%): C, 35.06; H, 3.23; N, 4.69. MW: 1115.52 g/mol. Molar conductivity: 64.6 $\Omega^{-1}cm^2mol^{-1}$. FT-IR spectroscopy (ATR, cm^{-1}): 3331 m,br ν(OH+NH), 3065 m ν(CH_{arom}), 2902 m ν(CH_{aliph}), 1639 m ν(C=N), 1605 m ν(C=C), 1570 m, 1509 m, 1369 m, 1281 m, 1198 m ν(C–O), 1126 s, 1032 m, 989 m, 887 m, 842 m δ(CH_{arom}), 695 m, 676 m, 572 m, 524 m, 425 m, 406 m. ^{1}H-NMR spectroscopy (500 MHz, ppm): 13.91 s (1H, NH), 8.27 s (1H, H5), 7.86 s (1H, H7), 7.80 d (1H, J=3.0, H3'), 7.10 dd (1H, J=9.0, 3.0, H5'), 7.04 d (1H, J=9.0, H6'), 3.82 s (3H, OCH_3). Fluorescence spectroscopy (λ, nm): 395 m,br, 417 m,br.

Determination of antimicrobial activity

Antimicrobial activity against *Staphylococcus aureus ATCC 6538*, *Staphylococcus epidermidis ATCC 12228*, *Escherichia coli ATCC 8739*, *Klebsiella pneumoniae ATCC 4352*, *Pseudomonas aeruginosa ATCC 27853*, *Proteus mirabilis ATCC 14153* (bacteria) and *Candida albicans ATCC 10231*, *Candida parapsilosis* ATCC 22019 and *Candida tropicalis* ATCC 750 (fungi) were determined by the microbroth dilutions technique following the Clinical and Laboratory Standards Institute (CLSI) recommendations.[36,37] Mueller-Hinton broth (MHB) (Difco) for bacteria, RPMI-1640 medium buffered to pH 7.0 with MOPS (Sigma) for yeast strain was used as the test medium. Serial two-fold dilutions ranging from 5000 μg/mL to 2.4 μg/mL were prepared in MHB. The inoculum was prepared using a 4–6 h broth culture of each bacteria and 24 culture of yeast strains adjusted to a turbidity equivalent to a 0.5 McFarland standard, diluted in broth media to give a final concentration of 5×10^5 cfu/mL for bacteria and 0.5×10^3 to 2.5×10^3 cfu/mL for yeast in the test tray. To prevent evaporation of the solvent, trays were covered and placed in plastic bags. The trays containing MHB were incubated at 35°C for 18–20 h and the trays containing RPMI-1640 medium were incubated at 35ºC for 46–50 h. The minimum inhibitory concentrations (MIC) were defined as the lowest concentration of compound giving complete inhibition of visible growth. Antimicrobial effects of dimethylsulfoxide (DMSO) were investigated against test microorganisms as control. Ciprofloxacin and Amphotericin B were used as reference antimicrobials to verify the standardization of the microdilution test procedure for bacteria and yeast, respectively. According to values of the controls, the results were evaluated. The MIC values of the Ciprofloxacin and Amphotericin B were within the accuracy range in CLSI throughout the study.[38] The experiments were carried out in duplicate.

CONCLUSIONS

In this study, six new benzimidazolylphenol derivatives, 2-[4,6-{Dichloro/dimethyl/bis-(trifluoromethyl)}-benzimidazol-2-yl]-(5-bromo/ methoxy)-phenols (**HL_1** – **HL_6**) and their complexes with $ZnCl_2$, $PdCl_2$ and $AuCl_3$ were synthesized and characterized using analytical techniques and modern spectroscopic methods. It was observed that the complexes have generally 1:2 M:L ratio and the metal centers are four coordinated. The gold(III) complexes are 1:1 electrolyte whereas the others are non-electrolyte according to the molar conductivity measurements. The fluorescence spectral data showed that the electronegative substituents such as bromo, chloro, trifluoromethyl and methoxy increased redshift. The highest wavelength was exhibited by trifluoromethyl-methoxy derivative (**HL_6**) with a maximum

wavelength such as 531 nm among the ligands. In the complexes, decreasing in red-shifting and fluorescence intensity was observed compared to the ligands. In addition, antimicrobial activity of the compounds was evaluated against six bacteria and three fungi. The gold(III) complexes showed superior antibacterial activity, while the palladium(II) complexes were found to be more effective against fungi than the ligands and metal salt.

Acknowledgments. This work was supported by Scientific Research Projects Coordination Unit of Istanbul University-Cerrahpasa. Project number: 23116.

REFERENCES

1. X.-J. Fang, P. Jeyakkumar, S. R. Avula, Q. Zhou and C.-H. Zhou, *Bioorg. Med. Chem. Lett.*, **2016**, *26*, 2584–2588.
2. M. Marinescu, D. G. Tudorache, G. I. Marton, C.-M. Zalaru, M. Popa, M.-C. Chifiriuc, C.-E. Stavarache and C. Constantinescu, *J. Mol. Struct.*, **2017**, *1130*, 463–471.
3. R. Abraham, P. Prakash, K. Mahendran and M. Ramanathan, *Microb. Pathog.*, **2018**, *114*, 409–413.
4. R. Sharma, A. Bali and B. B. Chaudhari, *Bioorg. Med. Chem. Lett.*, **2017**, *27*, 3007–3013.
5. E. Menteşe, F. Yılmaz, M. Emirik, S. Ülker and B. Kahveci, *Bioorg. Chem.*, **2018**, *76*, 478–486.
6. M. A. Tantray, I. Khan, H. Hamid, M. S. Alam, A. Dhulap and A. Kalam, *Bioorg. Chem.*, **2018**, *77*, 393–401.
7. Y. Bansal and O. Silakari, *Bioorg. Med. Chem.*, **2012**, *20*, 6208–6236.
8. R. Bonnett, *Chem. Rev.*, **1963**, *63*, 573–605.
9. N. G. Brink and K. Folkers, *J. Am. Chem. Soc.*, **1950**, *72*, 4442–4443.
10. M. Rasschaert, D. Schrijvers, J. van den Brande, J. Dyck, J. Bosmans, K. Merkle and J. B. Vermorken, *Br. J. Cancer*, **2007**, *96*, 1692–1698.
11. M. Montillo, F. Ricci, A. Tedeschi, E. Vismara and E. Morra, *Expert Rev. Hematol.*, **2010**, *3*, 131–148.
12. M. Bergmann, M. Goebeler, M. Herold, B. Emmerich, M. Wilhelm, C. Ruelfs, L. Boening and M. Hallek, *Haematologica*, **2005**, *90*, 1357–1364.
13. M. Michael, I. Bruns, E. Bölke, F. Zohren, A. Czibere, N. N. Safaian, F. Neumann, R. Haas, G. Kobbe and R. Fenk, *Eur J Med Res.*, **2010**, 29, 13–19.
14. A. Heider and N. Niederle, *Anti-Cancer Drugs*, 2001, 12, 725–729.
15. M. Rasschaert, D. Schrijvers, J. Van den Brande, J. Dyck, J. Bosmans, K. Merkle and J. B. Vermorken, *Br. J. Cancer*, **2007**, *96*, 1692–1698.
16. E. H. Hashem and Y. El Bakri, *Arab. J. Chem.*, **2021**, *14*, Article ID 103418.
17. A. Tavman, M. Hacioglu, D. Gürbüz, A. Cinarli, M.A.F. Oksüzömer and A. S. Birteksöz Tan, *Bull. Chem. Soc. Ethiop.*, **2019**, *33*, 451–466.
18. E. Alterhoni, A. Tavman, M. Hacioglu, O. Şahin and A. S. Birteksöz Tan, *J. Mol. Struct.*, **2021**, *1229*, Article ID 129498.
19. A. Tavman, D. Gürbüz, Ş. Öksüz and A. Çinarli, *Mor. J. Chem.*, **2018**, *6*, 328–341.
20. A. Tavman, A. Çınarlı, D. Gürbüz and A. S. Birteksöz, *J. Iran. Chem. Soc.*, **2012**, *9*, 815–825.
21. A. Tavman, S. Ikiz, A.F. Bagcigil, Y.N. Ozgür and S. Ak, *J. Serb. Chem. Soc.*, **2009**, *74*, 537–548.
22. R. Sathyanarayana, V. Kumar, G.H. Pujar, B. Poojary, M. K. Shankar and S. Yallappa, *J. Photochem. Photobiol. A: Chem.*, **2020**, *401*, Article ID 112751.
23. K. Akutsu-Suyama, S. Mori and T. Hanashima, *Photochem. Photobiol. Sci.*, **2019**, *18*, 2531–2538.
24. M. Barwiolek, A. Wojtczak, A. Kozakiewicz, M. Babinska, A. Tafelska-Kaczmarek, E. Larsen, E. Szlyk, *J. Lumines.*, **2019**, *211*, 88–95.
25. A. Tavman, A. S. Birteksöz and F. Öksüzömer, *S. Afr. J. Chem.*, **2012**, *65*, 150–158.
26. W. Geary, *J. Coord. Chem. Rev.*, **1971**, *7*, 81–122.
27. K. Nakamoto, Infrared and Raman Spectra of Inorganic and Coordination Compounds, Part B, 5th ed., **1997**, John Wiley and Sons, Inc.: New York.
28. S. Abbate, G. Longhi, G. Mazzeo, C. Villani, S. Petković and R. Ruzziconi, *RSC Adv.*, **2019**, *9*, 11781–11796.
29. A. E. Özel, S. Kecel and S. Akyüz, *J. Mol. Struct.*, **2007**, *834–836*, 548–554.
30. V. T. Yilmaz, S. Hamamci, Ö. Andac, K. Güven, *Z. Anorg. Allg. Chem.*, **2003**, *629*, 172–176.
31. X.-F. Yang, H. Qi, L. Wang, Z. Su, G. Wang, *Talanta*, **2009**, *80*, 92–97.
32. M. Mosquera, M. C. R. Rodríguez, F. Rodriguez-Prieto, *J. Phys. Chem. A*, **1997**, *101*, 2766–2772.
33. F. Rodriguez-Prieto, J. C. Penedo, M. Mosquera, *J. Chem. Soc. Faraday Trans.*, **1998**, *94*, 2775–2782.
34. H.F. Ridley, G.W. Spickett,and G.M. Timmis, *J. Het. Chem.*, **1965**, *2*, 453–456.
35. A. Tavman, *Spectrochim. Acta A*, **2006**, *63*, 343–348.
36. Clinical and Laboratory Standards Institute (CLSI). Methods for dilution antimicrobial susceptibility tests for bacteria that grow aerobically: Approved Standard M7-A5, **2006**, Wayne, PA: USA.
37. Clinical and Laboratory Standards Institute (CLSI). Reference method for broth dilution antifungal susceptibility testing of yeasts: Approved Standard M27-A2, 2nd ed., **2002**, Clinical Laboratory Standards, Wayne, PA: USA.
38. Clinical and Laboratory Standards Institute. Performance standards for antimicrobial susceptibility testing; 24th informational supplement. M 100-S24:CLSI, **2014**, Wayne, PA: USA.